JABFM
eISSN 2280-8000

J Appl Biomater Funct Mater 2016; 14(1): e42-e52
DOI: 10.5301/jabfm.5000249

ORIGINAL ARTICLE

Bioactive TGF-β1/HA alginate-based scaffolds for osteochondral tissue repair: design, realization and multilevel characterization

Luca Coluccino[1,2], Paola Stagnaro[3], Massimo Vassalli[4], Silvia Scaglione[1]

[1] IEIIT Institute, CNR–National Research Council of Italy, Genoa - Italy
[2] Nanophysics Department, Italian Institute of Technology, Genoa - Italy
[3] ISMAC Institute, CNR–National Research Council of Italy, Genoa - Italy
[4] IBF Institute, CNR–National Research Council of Italy, Genoa - Italy

ABSTRACT

Background: The design of an appropriate microenvironment for stem cell differentiation constitutes a multitask mission and a critical step toward the clinical application of tissue substitutes. With the aim of producing a bioactive material for orthopedic applications, a transforming growth factor-β (TGF- β1)/hydroxyapatite (HA) association within an alginate-based scaffold was investigated. The bioactive scaffold was carefully designed to offer specific biochemical cues for an efficient and selective cell differentiation toward the bony and chondral lineages.
Methods: Highly porous alginate scaffolds were fabricated from a mixture of calcium cross-linked alginates by means of a freeze-drying technique. In the chondral layer, the TGF in citric acid was mixed with an alginate/alginate-sulfate solution. In the bony layer, HA granules were added as bioactive signal, to offer an osteoinductive surface to the cells. Optical and scanning electron microscopy analyses were performed to assess the macro-micro architecture of the biphasic scaffold. Different mechanical tests were conducted to evaluate the elastic modulus of the grafts. For the biological validation of the developed prototype, mesenchymal stem cells were loaded onto the samples; cellular adhesion, proliferation and in vivo biocompatibility were evaluated.
Results and conclusions: The results successfully demonstrated the efficacy of the designed osteochondral graft, which combined interesting functional properties and biomechanical performances, thus becoming a promising candidate for osteochondral tissue-engineering applications.

Keywords: Alginate, Biomaterial, Hydroxyapatite, Scaffold, Tissue engineering, Transforming growth factor beta 1

Introduction

One of most challenging battles of tissue engineering is the realization of bioactive materials able to avoid tissue disease and degeneration, as well as trauma in young and active people (1-4). Scaffolds properly designed starting from such bioactive materials should in principle offer the appropriate biomechanical performances besides inducing tissue regeneration in vivo.

In particular, considering the intrinsically distinct structural, biochemical and functional features of strictly connected tissues, such as the articular cartilage/subchondral bone system, several research groups have addressed their efforts to the development of "osteochondral" composite materials consisting of 2 different components, representing the 2 natural tissues (5-10).

As regards bone, engineered scaffolds need to possess the proper mechanical properties (i.e., structural integrity, stiffness, strength) to stand physiological loading, combined with a controllable degradation rate to guarantee long-term tissue regeneration (11-13). Among the several materials studied, porous scaffolds based on degradable polymers, either natural or synthetic, such as poly(lactic-*co*-glycolic acid), collagen, polycaprolactone and silk, are those that could meet these requirements (11, 14-17).

On the other hand, it was shown that hydrogels obtained from polymers, such as poly(ethylene glycol), agarose, alginate and chitosan, better mimicking the natural environment of cartilage tissue, can well support chondrocyte culture and differentiation (18-21).

However, the mechanical performance of these engineered tissues is often poor (22). For an improved mechanical performance of engineered osteochondral tissue, the

Accepted: April 25, 2015
Published online: December 25, 2015

Corresponding author:
Luca Coluccino
IIT - Nanophysics Department
Via Morego 30
16163 Genova, Italy
Luca.Coluccino@iit.it
luca.coluccino@ieiit.cnr.it

realization of 3-dimensional (3D) *bilayered*, but at the same time, *monolithic* structures, guaranteeing overall structural integrity of the graft, could represent a promising alternative to overcome the limitations of weak interface between the 2 distinct layers (bony and chondral ones). Some authors have recently developed a monolithic biphasic scaffold realized in polycaprolactone and successfully tested its mechanical and functional performance (23).

In recent years, natural polymers have been widely proposed as promising alternatives to synthetic materials, due to their biological properties of interest for numerous medical applications (24). In particular, various polysaccharides can easily form hydrogels with a 3D structure that mimics the extracellular matrix (ECM) of connective tissues participating in several biological reactions in vivo (25). Among them, alginic acid is a linear copolymeric polysaccharide consisting of β-D-mannuronic (M) and α-L-guluronic (G) acid residues arranged in M-rich blocks, G-rich blocks, and alternating or random sequences of M and G units. Overall, the copolymer composition, relative amount of each block type, and molecular weight depend on its algal or bacterial origin (26, 27).

Water-soluble sodium salt of alginic acid displays the great ability of giving highly viscous solutions even at moderate concentrations; this property has been exploited in food processing, pharmacology, drug delivery and 3D supporting of specific cell culture such as chondrocytes (28).

Moreover, water-stable relatively tough hydrogels can be easily achieved from sodium alginate grades with high content of G units by partial replacement, through ionic exchange, of Na^+ counter ions with alkaline-earth ions, such as Ca^{2+}, and formation of strong ionic cross-links due to the preferential interaction of the G-rich blocks with the divalent cations (26).

In the present work, with the aim of producing a highly porous bilayered scaffold functionalized for osteochondral tissue regeneration, an alginate-based monolithic prototype was developed using the freeze-drying technique. The 3D structure was carefully designed varying the concentrations of sodium alginate and calcium cross-linker to have adequate mechanical properties, while favoring an enhanced in vivo cell-mediated matrix deposition.

To generate a bioactive scaffold capable of inducing a cellular differentiation, 2 specific biochemical signals were introduced: respectively, a mineral phase, i.e., hydroxyapatite (HA), in the bony layer, and a transforming growth factor (namely, TGF-β1) in the chondral layer. While HA is a widely used ceramic compound mimicking the mineral phase of bone tissue (5, 10, 29-33), TGF-β1 is known to play a key role in chondrocyte proliferation, differentiation and ECM production (34-36).

Micro-macro architecture of the highly porous alginate-based scaffold was assessed by SEM morphological characterization and porosity analysis. Thermal and long-term stability under pseudophysiological conditions were investigated. Uniaxial compressive mechanical tests and atomic force microscopy (AFM) imaging measurements were conducted to evaluate the elastic modulus. In vitro and in vivo tests were performed by using mesenchymal stem cells (MSCs) to evaluate the capability of the bioactive scaffold of inducing a selective cellular differentiation and eventually supporting matrix deposition and mature tissue regeneration.

Materials and methods

Preparation of the bioactive alginate-based scaffolds

Two different sodium alginate solutions were prepared by mixing either 1% or 2% (w/v) of Keltone LV Alginate (Kelco Co., San Diego, CA, USA) solution with 1% or 2% (w/v) of Alginate LVG (Pronova Biomedical, Norway) solution, respectively, finally obtaining 2% or 4% (w/v) of total sodium alginate concentration in a 0.154 M NaCl solution. The effective intimate mixing of the alginate solutions required 12 hours at room temperature under vigorous magnetic stirring. The solutions were then stored at a temperature of 4°C.

Cylindrical specimens of alginate-based scaffolds were made as follows: a mold of agar gel, 1% (w/v) of DIFCO Agar powder in a 0.154 M NaCl solution, enriched with $CaCl_2$ (J.T. Baker), as the alginate cross-linking agent, was prepared. Two different molarities of the $CaCl_2$ cross-linker in physiological solution were prepared and tested: 0.3 and 0.5 M. A volume of 2-mL alginate solution was then introduced into the mold by a syringe; the gelification process was allowed to take place at 37°C for at least 3 hours, to ensure a complete diffusion of calcium ions from the agar mold to the alginate solution (Fig. 1). Alginate hydrogels thus formed were then removed from the mold and frozen for 12 hours at -20°C. The final highly porous structure was generated by the freeze-drying technique (-50°C, 1 mbar for 48 hours).

Alginate-based scaffolds were bioactivated with HA powder (kindly provided by Finceramica Faenza) and with the TGF-β1 (LiStarFish, Milano, Italy) to induce, respectively, osteogenic and chondrogenic differentiation as well as ECM deposition.

For the preparation of the bone-like layer, the required amount of HA powder was mixed with sodium alginate powder (HA to alginate ratio 1/5 w/w) before preparing the solution.

For the preparation of the chondral-mimicking layer, TGF-β1 was reconstituted in citric acid (10 mM, pH 3) as previously described (37). Sodium alginate-sulfate was synthesized from the sodium alginate to sustain TGF-β1 chemical linkage to the alginate scaffold.

For the alginate sulfation, a synthetic method already described (26) was modified as follows: 1.0 g of sodium alginate (molecular weight [MW] $2 \div 3 \times 10^5$ Da, G unit content 60%) was added to a solution of 2 mL $ClSO_3H$ (>98%; Fluka) in 8 mL formamide (99.5%; Aldrich). The sulfation reaction was completed by maintaining the mixture at 60°C for 4 hours. Afterwards, 50 mL acetone was added to precipitate the sulfated alginic acid, the precipitate was dissolved in distilled water, the pH was adjusted to 10-11 by adding NaOH 0.1 M, and the resultant sulfate-alginate solution was dialyzed for 72 hours through a membrane with a cutoff of 12×10^3 Da. The product, obtained at a yield of 65%, was characterized by Fourier transform infrared (FTIR) and nuclear magnetic resonance (NMR) spectroscopy.

The bioactive factor was then incubated with the alginate-sulfate solution for 1.5 hours at 37°C. An amount of 32 µL of TGF-β1 solution (50 µg/mL) in citric acid was directly added to 2 mL of calcium cross-linked alginate/alginate-sulfate solution, previously prepared mixing 1.8 mL of 2% (w/v) of sodium alginate and 0.18 mL of 2.5% (w/v)

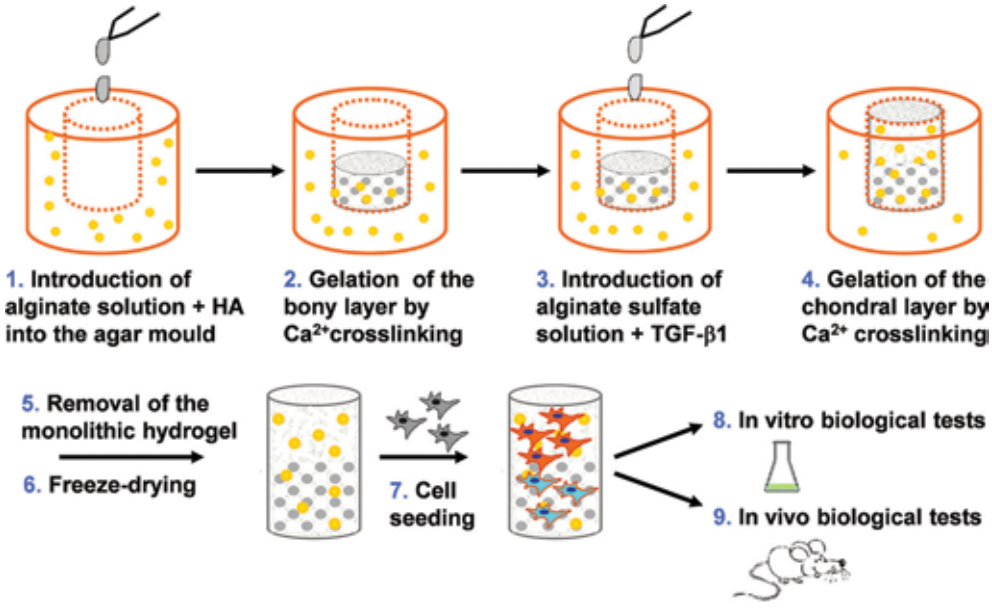

Fig. 1 - The overall alginate-based bilayered scaffold preparation process: an agar gel plate added by the alginate cross-linker is used as a mold for the alginate hydrogel gelification, gelation, other term for gelification: creation of a gel and the subsequent freeze-drying leads to the final porous scaffolds. HA = hydroxyapatite.

of alginate-sulfate. The final amount of TGF-β1 for each sample (cubes with 3-mm sides) was 200 ng, as previously reported (37).

Morphological and structural analysis: scanning electron microscopy and porosity evaluation

Morphology and microstructure of the alginate-based scaffolds, after the freeze-drying process, were analyzed both by optical (OM) and scanning electron (SEM) microscopy, performed, respectively, on a Nikon Ni-U OM and on an Hitachi TM 3000 operating at 10 ÷ 15 kV acceleration voltage and equipped with a EDX SwiftED3000 probe (Oxford Instruments). Before SEM observation, the freeze-dried samples were completely dehydrated with ethanol, mounted on aluminium stubs and sputter-coated with gold. Acquired SEM images were then elaborated with the open source software GIMP 2.0 to evaluate the mean pore size (calculated from 16 measurements for each sample).

A rough estimation of the scaffold percentage specimen porosity (P) was done, using the following equation:

$$P = \left[1 - \frac{density\ of\ scaffold}{density\ of\ solid\ material}\right] * 100 \qquad \text{Eq. [1]}$$

where density of scaffold is calculated as the ratio between the weight and the volume of specimens cut in a regular shape, and density of solid material is the tabulated bulk density of sodium alginate (1.6 g cm^{-3}).

Thermogravimetric analysis

Thermal stability of the alginate-based scaffolds was investigated by thermogravimetric analysis (TGA) carried out with a TGA7 (Perkin Elmer) instrument under nitrogen atmosphere (40 mL/min gas flow rate) on previously freeze-dried samples of about 10 mg. Dynamic TGA experiments were performed heating the specimens from 50°C up to 700°C at the rate of 20°C/min. At 700°C, oxygen was introduced in the instrument furnace, and the inorganic residue was determined at 880°C. Before starting the heating run, the samples were kept at 50°C for 10 minutes to stabilize their initial weight.

FTIR and NMR spectroscopy

FTIR spectra of the pristine sodium alginate and the synthesized sodium alginate-sulfate were recorded on a Bruker IFS 28 FTIR spectrophotometer in the normal transmission mode (32 scans, resolution 4 cm^{-1}, wave number range 4,000-400 cm^{-1}) using the KBr method. The ^{1}H and ^{13}C NMR spectra of the above mentioned samples were recorded in D_2O at 50°C on a Mercury 300BB Varian spectrometer.

Mechanical analysis: unconfined compression and stress relaxation tests

The evaluation of the compressive strength of the alginate scaffolds in a dry and wet state was performed by using a benchtop mechanical tester (Zwick All Round Z005; Zwick Roell Italia) using a load cell of 100 N, with preload 0.5 N (dry samples) or 0.1 N (wet samples). The specimens were cylinders of about 8 mm in thickness and 6-8-mm diameter. The crosshead speed of the tester in the compressive tests was set at 0.4 mm/min, and load was applied until an 80% reduction in specimen height. Mechanical parameters were measured on several identical specimens, and the average values were calculated.

A dynamic mechanical analyzer (DMA) Q800 (TA Instrument, USA) was used for the stress relaxation tests. For the DMA analysis, 2 cycles of compression were performed on the samples in the dry and wet state (Phosphate-Buffered Saline (PBS) solution at 37°C), reaching 5% and 10% of strain to measure the material stress relaxation ability while keeping constant the deformation state for 10 minutes.

Atomic force microscopy

AFM imaging and nanoindentation were performed using an Asylum MFP-3D system; samples were prepared as for the mechanical analysis (see previous paragraph). Imaging was performed in contact mode using rectangular cantilevers with a silicon dioxide tip (Spring constant 27.85 N/m) that were calibrated using Sader's method (38). In addition, an elasticity map was obtained on selected samples by performing full indentation curves (scan area 15 × 15 μm^2, scan rate 0.80 Hz). The value of the elastic modulus was extracted on application of the Hertz model on the indentation part of each curve.

Degradation study

To evaluate the in vitro alginate degradation, 6 parallel samples of 560 ± 215 mg each were suspended in 14 mL of PBS and incubated at 37°C and 5% CO_2 for 2 months; periodically an aliquot of solution was withdrawn and analyzed at λ = 230 nm using a Varian Cary 400 BIO spectrophotometer. The absorbance of the withdrawn solution was proportional to the concentration of degradation products being formed, normalized to the time-varying volume.

Cell adhesion and viability

Bone marrow aspirate of a female Fisher rat (4 weeks old) was harvested from the 2 femurs of the animal with approval of competent ethical committee and legal authorities.

Bone marrow samples were collected in a sterile tube, washed twice with PBS and suspended in Dulbecco's modified Eagle's medium (DMEM) supplemented with 10% fetal calf serum (FCS), 100 IU/mL penicillin and 100 mg/mL streptomycin and plated at a density of 10^6 cells/cm^2. Each cell culture was maintained in an atmosphere of 5% CO_2 in air at 37°C.

Medium was changed 2 days after the original plating and then twice a week. When culture dishes were nearly confluent (passage 0), bone marrow–derived MSCs, were detached with 0.05% trypsin-0.01% EDTA and replated with a density of 3,000 cells/cm^2 (passage 1) until the next confluence.

When they had reached the necessary number, MSCs were counted, resuspended at a concentration of 10^6 cells in 100 µL, and seeded onto alginate scaffold specimens (3 × 3 × 3-mm^3 size) for biological tests. After 1 hour, additional medium was added onto each sample. The scaffolds were previously sterilized by gamma rays (5,000 rad).

The cell constructs were cultivated at 37°C, in a 5% CO_2 humidified incubator. After 24 hours, some samples were washed in PBS, fixed in 4% paraformaldehyde for 2 hours, and rinsed in PBS. Samples were subsequently stained with hematoxylin for 5 minutes to evaluate cell adhesion on both the internal and external surface of the biomaterial.

The viability of MSCs cells cultured on the alginate scaffolds was determined after 1, 3 and 7 days with with Live/Dead® assay kit, purchased from Invitrogen. Briefly, alginate scaffolds were rinsed in PBS and then seeded with 0.75 × 10^6 cells per scaffold in a phenol red-free medium. After 24 hours, the scaffolds were incubated with 150 µL of Live/Dead staining solution at 37°C for 30 minutes. The images for the 3 different channels (green, red and brightfield) were taken with a fluorescence microscope (Olympus IX70) and then postprocessed using NIH ImageJ Software. The amount of live (green channel) and dead cells (red channel) was analyzed, merging the 2 fluorescence images into a composite stack and calculating the percentage of viability from the 2 fluorescence channel distributions.

The same procedure was performed on days 3 and 7.

In vivo functional tests

Four-week-old female Fischer 344 rats (F344) were anesthetized by intraperitoneal injection of Sodium Pentothal at a final concentration of 3 mg/100 g of body weight. The hair of the rat was cut at the implantation area, followed by washing with tap water, and scrubbed with tincture of iodine. In each rat, 4 skin incisions on the back were made. Alginate-based constructs were implanted subcutaneously into the respective pocket and skin sutured. As a negative control, alginate scaffolds without rat bone marrow mesenchymal stem cells (RBMSCs) were used. After 2 weeks of implantation, the animals were sacrificed with CO_2, and the implants were retrieved.

Explants were fixed in 4% paraformaldehyde, decalcified with Osteodec solution (Bioptica, Italy) and processed for histological analysis. First, the constructs were dehydrated in an ascending series grade ethanol/water solution (from 70% to 100%) followed by 2 washing with xylene. Then, specimens were immersed in paraffin at 60°C. Slides were then prepared by cutting the specimens into sections 5-µm thick using a microtome. Paraffin was removed with xylene washing, followed by descendent series grade ethanol/water solution.

Slides were then stained with hematoxylin and eosin (H&E), and then mounted to avoid the formation of bubbles for observation. All slides were examined under an optical microscope (Nikon Ni-U, Japan).

Results and discussion

Structural analysis: SEM and scaffold porosity evaluation

The preparation of 3D porous scaffolds was realized as follows. First an agar mold was prepared by dissolving agar powder in a physiological solution containing calcium chloride. Then the alginate solution was introduced into wells cut in the agar mold. The alginate gelification process took place by migration of the calcium ions into the alginate solution. After the alginate hydrogel was well formed, it was removed from the agar mold and frozen at -20°C. The final porous structure was obtained by means of a controlled freeze-drying process (Fig. 1)

Using this manufacturing procedure, a monolithic 3D configuration was obtained using the same basic polymeric matrix for the overall osteochondral graft, while the bilayer structure was obtained by functionalizing the bony and chondral layers with bioactive signals (HA and TGF-β1, respectively).

This hydrogel preparation technique allows a tunable crosslinking degree, according to the specific gelification process, thus being able to influence the overall morphology of the 3D graft. The formation of an internal stretched porosity along a specific axis was obtained in those cases when the cross-linker diffusion was limited to the perimetral surface

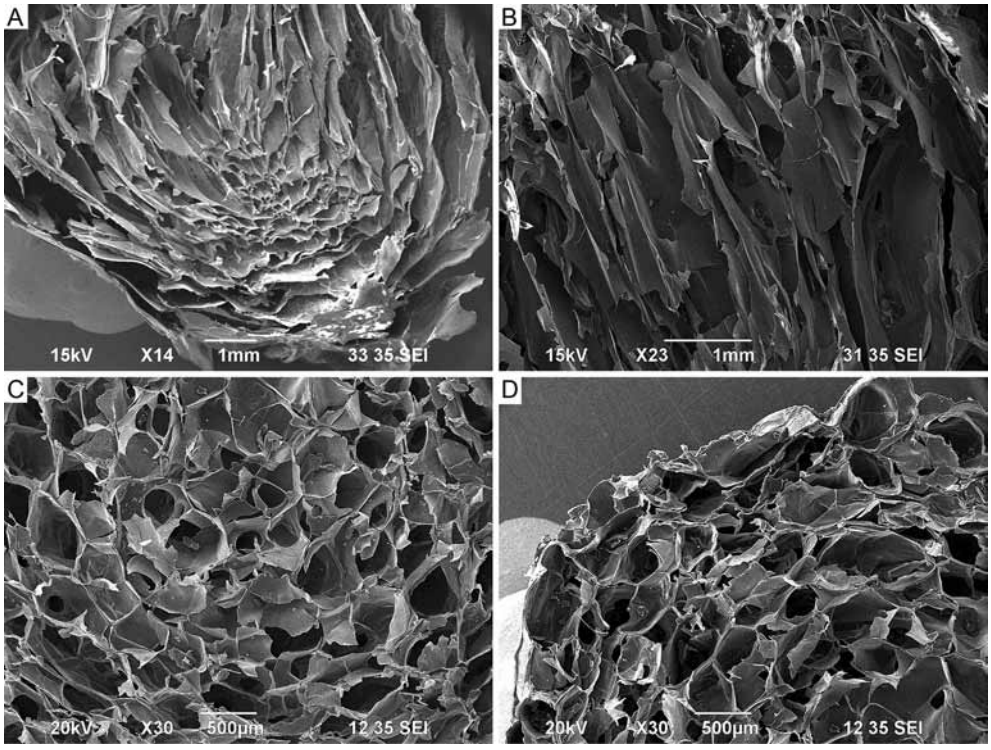

Fig. 2 - SEM images of the alginate freeze-dried scaffolds; it is possible to note the morphology of a stretched porosity within the bulk core given by directional tensions during nonhomogeneous gelification (**A, B**), and a homogeneous honeycomb-like porosity after a more isotropic diffusion of the cross-linker through the hydrogel (**C, D**).

(Fig. 2A, B), while the scaffold prototypes with the most spatial homogenization of the internal porosity were obtained by driving the cross-linker diffusion from every direction to the alginate core solution (Fig. 2C, D).

Scaffold structure and morphology was investigated by OM and SEM microscopy. From SEM micrographs, pore size distribution was calculated to verify the scaffold suitability for osteochondral regeneration. Most of the pores are in the range between 200 and 600 µm, and only 15% of the pores had a diameter more than 600 µm (Fig. 3), guaranteeing a high macro-porosity favoring a future ECM deposition (39). Moreover, a certain degree of pore interconnection is visible; indeed, the scaffold penetrability is important for vascularization and blood vessel invasion (39). A cell wall thickness of ca. 50 µm can be measured from SEM micrographs at higher magnifications. From the morphometric data analysis, it was found that the cross-linker concentration seemed to have a higher influence on the scaffold total porosity with respect to the sodium alginate concentration: indeed, increasing the concentration of cross-linking factor (0.3 M vs. 0.5 M) resulted in a decrease of total porosity (from 90.8% ± 1.5% to 81.3% ± 7.9%), while the sodium alginate concentration seemed not to have an appreciable influence on resultant scaffold porosity (data not shown).

Based on morphological and structural results, a prototype made up of 2% w/v of alginate concentration and a 0.3-M calcium cross-linker molarity agar mold were chosen.

Thermogravimetric analysis and long-term stability

TGA was carried out on the freeze-dried alginate-based scaffolds to evaluate their thermal stability. All of the TGA curves (not shown), recorded under nitrogen over a temperature range from 50°C to 700°C, had similar profiles and exhibited

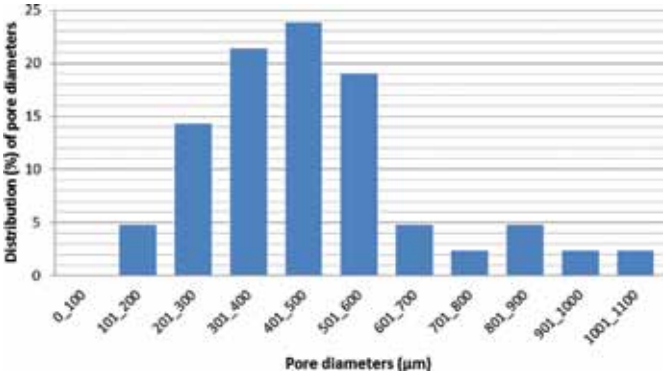

Fig. 3 - Pore diameter distribution of 2% w/v of alginate concentration scaffold with a cross-linker molarity of 0.3 M.

a multistep degradation behavior (40-43). The variable weight loss (ca. 15 and 8 wt.%, respectively, for calcium cross-linked alginate without and with HA samples) observed up to 105°C-110°C was due to the release of absorbed water; on heating up to about 220°C, dehydration reactions accompanied by formation of volatiles take place. In the temperature range from 220°C to 360°C, the polymer chain completely degrades in 2 steps forming a char, whose combustion, after the introduction of oxygen in the furnace at 700°C, yields an inorganic residue, likely made of carbonates and oxides of sodium and calcium, and HA, when present. In Table I, TGA results relative to calcium cross-linked alginate representative samples without and with HA are summarized. As expected, samples containing HA presented a higher amount of inorganic residue. The 2-step degradation profile (T_1 and T_2 peaks ~250°C and 320°C, respectively) observed for the alginate polymer could be ascribed

TABLE I - TGA results for freeze-dried samples of calcium cross-linked alginate* without and with HA† aged at 50°C for different times

Sample	Aging (days)	T_1 peak (°C)	T_2 peak (°C)	Residue at 700°C (wt%)	Residue at 880°C (wt%)
Alg-Na2%	0	248	316	46	37
Alg-Na2%	28	258	318	53	43
Alg-Na2%	35	271	321	48	34
Alg-Na2%+HA	0	250	323	63	50
Alg-Na2%+HA	21	250	314	67	55
Alg-Na2%+HA	28	255	321	65	54
Alg-Na2%+HA	35	250	318	55	46

HA = hydroxyapatite; TGA = thermogravimetric analysis.
*Sodium alginate solution 2 wt%; calcium chloride 0.5 M.
†HA 1/5 wt% with respect to the sodium alginate.

to the different behavior of the chain sequences depending on the fact that they more (G-rich sequences) or less (M-rich ones) closely interact with calcium ions in the cross-links of the ionic network.

To check the long-term stability of the investigated scaffold material, further TGA experiments were carried out on freeze-dried samples maintained for different times at 50°C in air in sealed vials. As one can observe from data reported in Table I, the thermal degradation behavior results were practically unaffected by aging times of up to 5 weeks.

The mass loss (%) of alginate scaffolds over time was determined as a measure of degradation.

After 1 week, about 50% of alginate was shown to be solubilized, in very fast degradative kinetics; at 1 month, the percentage of alginate weight loss was about 60%, reaching 70% after 2 months (Fig. 4). Further investigations on these materials will be addressed to analyzing in vivo degrading behavior of such materials where the major mechanism for degradation (in humans) is disintegration of the material due to the gradual exchange of gelling calcium ions with sodium, finally accelerating the scaffold hydrolysis.

Preparation and characterization of functionalized alginate scaffold prototypes

Although the crucial role of porosity features (i.e., pore size and shape) on cell–material interactions is known, it is recognized that pore architectures with tailored porosity need to be complemented by bone/cartilage-inducing agents to stimulate native tissue formation activity.

HA powders were therefore added in the bony layer, to enhance the osteoconductivity of the graft and to favor interfacing with the host tissue. A chemical and morphological analysis on the alginate scaffolds functionalized with HA was performed to evaluate the distribution of the HA particles into the bulk material (Fig. 5). At low magnification, it was possible observe HA granules homogeneously distributed within the alginate-based graft (Fig. 5A). From a chemical point of view,

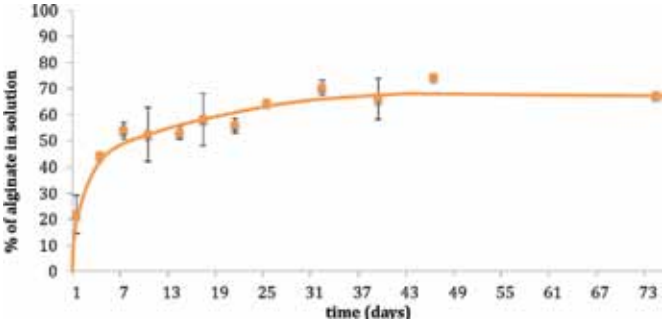

Fig. 4 - Weight loss of the alginate scaffolds during more than 2 months of incubation in phosphate-buffered saline (PBS) at 37°C.

the phosphorous (P) ion was mapped on the surface of both pure alginate and HA functionalized scaffolds (Fig. 5B). It was possible to observe a homogeneous spatial distribution of P in the HA-alginate scaffolds, confirming the presence of the exposed HA particles within the grafts. On the other side, the Ca/P ratio could not be measured, since calcium ions are present in both samples in the cross-linker used during the process.

As regards the functionalization of the scaffold layer designed for chondral regeneration, TGF-β1 was used as biochemical signal for cells, according to previously reported data (37). The binding of TGF-β1 to the porous alginate scaffold was guaranteed by using a combination of alginate/alginate-sulfate. Indeed, the incorporation of this growth factor into the properly functionalized (see below) 3D structure enabled its release over time, tuned with the cell differentiation and proliferation process.

In a previous work, Freeman et al (44) fabricated hydrogels made of mixed alginate/alginate-sulfate by sulfation reaction of the uronic acids units along the polysaccharide chains, to give them a specific affinity for heparin-binding proteins, such as growth factors. Indeed, in nature, the specific binding to heparin or heparan sulfate glycosaminoglycans (complex acidic polysaccharides found on the cell surface and in the ECM) (45) stabilizes and protects the growth factors from denaturation and proteolytic degradation (26). In our bilayered prototype, part of the sodium alginate was sulfated with the aim of bioactivating the scaffold layer destined to chondrogenesis by binding TGF-β1 to it. Sodium alginate-sulfate was prepared by sulfation of a commercial sodium alginate grade containing at least 60% of guluronic acid units; the reaction was carried out with chlorosulfonic acid in formamide, slightly modifying a method reported in the literature (26, 46). In Figure 6 the FTIR spectra of sodium alginate before and after sulfation reaction are compared.

Effective sulfation of the uronic units was testified to by the appearance in the reaction product FTIR spectrum, of the characteristic strong absorbance band relative to the symmetric stretching of the sulfur-oxygen double bond at about 1,250 cm^{-1}, accompanied by a weaker band at 800 cm^{-1} due to the S–O–C stretching (40). The ^{1}H and ^{13}C NMR spectra (not shown) confirmed the formation of the alginate-sulfate as revealed, in particular, by the shifting to lower fields of the signals related, respectively, to H-2 and H-3 protons and C-2 and C-3 carbons of the uronic units, due to the substitution

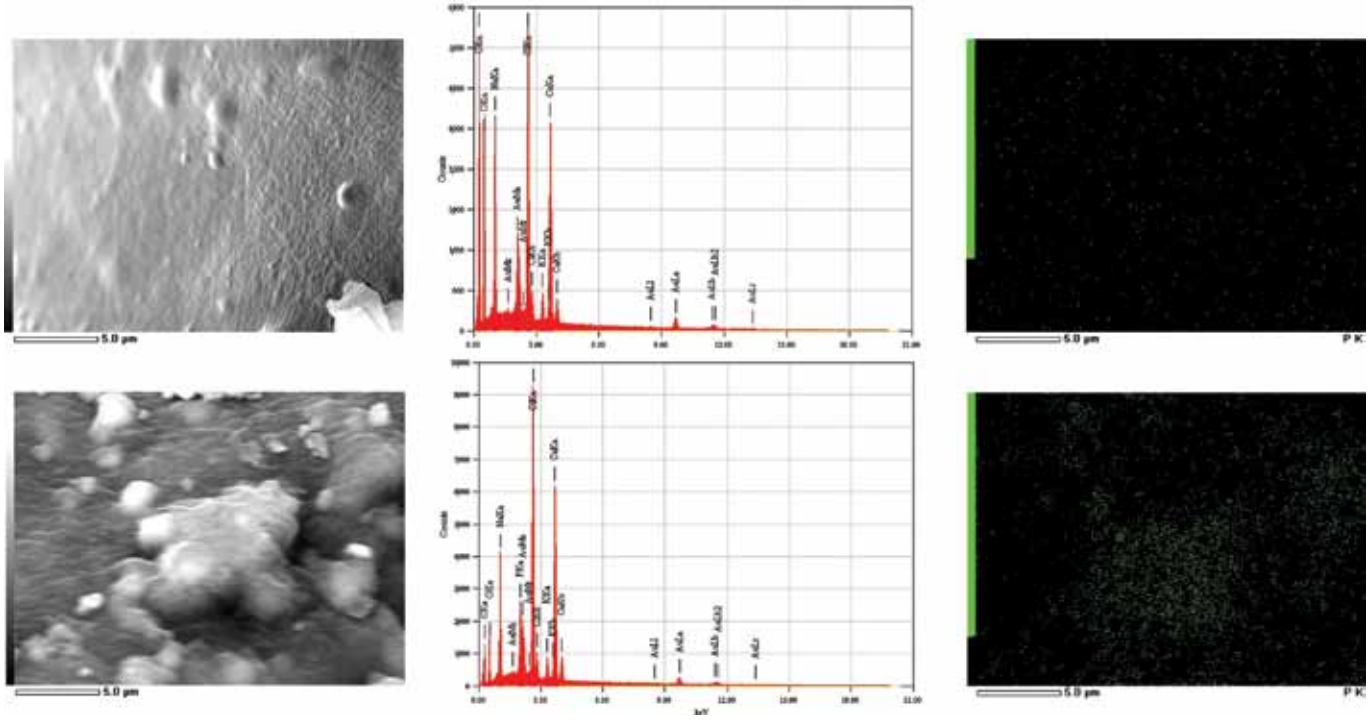

Fig. 5 - (**A**) Optical microscopy image of hydroxyapatite (HA) granules homogeneously dispersed within the alginate scaffold; (**B**) the EDX spectra of alginate and HA-alginate scaffolds. Mapping of chemical elements shows the spatial density of P (green dots) in both samples.

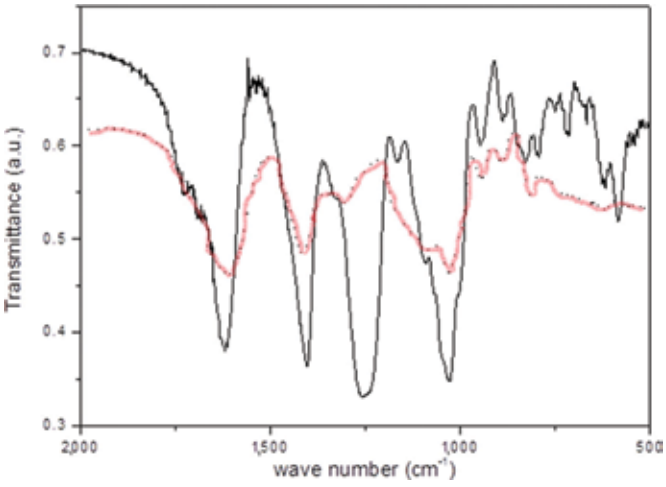

Fig. 6 - Fourier transform infrared (FTIR) spectra of sodium alginate (dotted line) and sodium alginate-sulfate (solid line). a.u. = arbitrary units.

of the hydroxyl groups with the electronegative sulfate ester groups, in good agreement with literature data for alginate (26) and alginate-sulfate (44).

Biomechanical analysis: AFM, unconfined compression and stress relaxation tests

The AFM study on the alginate scaffolds aimed to provide an evaluation of the stiffness of the material bulk, avoiding the porosity effects. We chose for this analysis to study the single walls of the pores, trying to compress them as much as possible on a general glass microscope slide.

A 15 × 15-μm morphological map was produced by this study, with its related stiffness map; there was found to be a good correspondence between 2 levels: the morphological profile and the mechanical one. Some artefacts, probably depending on the presence of salts on the surface, were found on both the maps, confirming the spatial correspondence between the 2 levels (Fig. 7A, B): most of the values of the indentation stiffness of the material were found to be in the range of 380-480 MPa.

For the overall influence of all manufacturing parameters on the 3D scaffolds' biomechanical behavior, a compression test was performed on a macro scale reaching 80% of the samples' capacity to tolerate the strain (Fig. 8A). The graph shows that there was a good correspondence between alginate concentration and mechanical properties: the 4% w/v alginate samples appeared to be stiffer than the ones at 2% w/v concentration.

The influence of cross-linking seemed to have less importance than the alginate content in the base solutions, even if it is clear that 0.5 M seemed to present a higher value of the compressive modulus, showing at the same time a comparable general mechanical behavior. The result for compressive modulus values was expected to be between 0.2 and 4.5 MPa (47); the average compressive stiffness of the alginate prototypes was 1.37 ± 0.717 MPa and so was successfully aligned with results in the literature.

The analysis at the DMA showed the viscoelastic behavior of alginate-based scaffolds, for the control group and for those activated with HA soaked in a PBS solutions at 37°C.

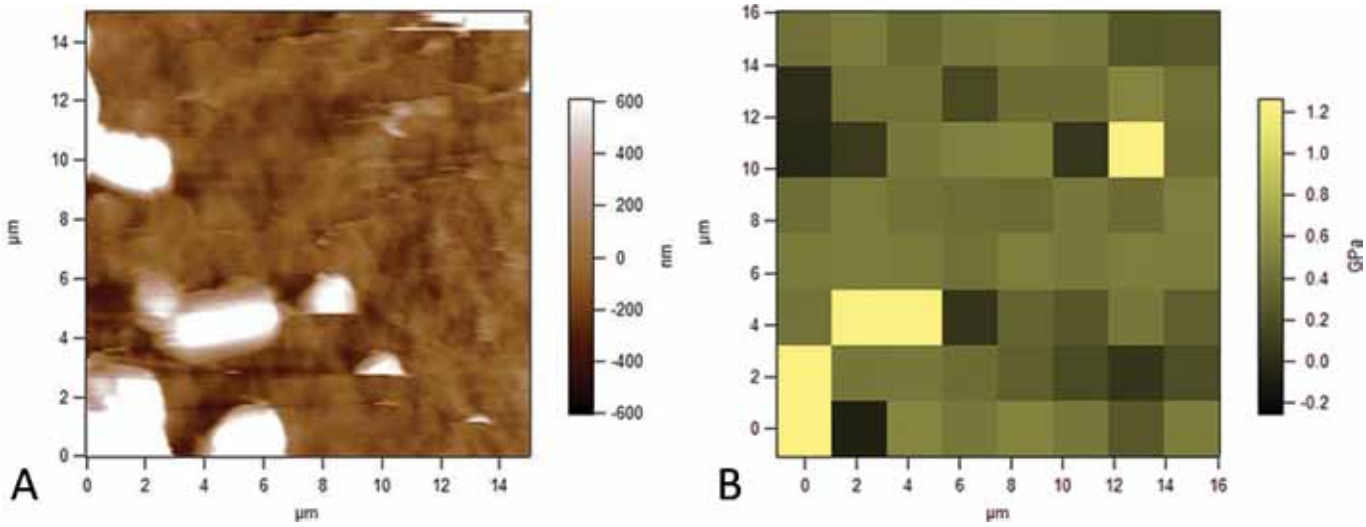

Fig. 7 - (**A**) Morphological map at the atomic force microscopy (AFM) of a 15 × 15 µm of alginate scaffold and its correspondent stiffness map (**B**). The resultant histogram of the compressive modulus distribution from the indentation stiffness tests.

The stiffness was measured in the first elastic phase of a compression cycle; the stress relaxation behavior was evaluated keeping constant the strain applied on the sample. The compressive modulus of alginate-HA scaffolds lost an order of magnitude when the samples were soaked in PBS solution, but the percentage of stress recovery ability was maintained generally on the same order (Fig. 8B). The presence of the water obviously affected the original strength of the internal architecture, decreasing the resistance to compression of the material, but the swelling capability did not affect the short-term stability of the structures.

Biological tests

The capability of cells to adhere to the alginate-based scaffolds and homogeneously colonize the 3D graft was macroscopically evaluated by toluidine blue staining. After 3 hours of culture, cells (in blue) were present along the entire depth and throughout the central region of the scaffolds with predominant staining of superficial layers (Fig. 9A). After 1 week of cell culture, grafts were fixed, and cellular adhesion evaluated. Cells were found to be well spread on the surface even at the inner part of the scaffolds (Fig. 9B).

Cell viability was found to be high based on Live/Dead staining (Fig. 10A-C): dead cells were found to be lower than 10% of the total cells stained, during the overall cell culture, proving the good biocompatibility of the alginate-based scaffolds and their limited cytotoxicity. The amount of live cells within the alginates during the period of observation (7 days) was quite constant, confirming the good biocompatibility of the graft. If compared with the traditional Petri dish cell culture, MSC proliferation on 3D alginate scaffolds was lower (data not shown), according to other previously published works (e.g., Scaglione et al (2010) (17), where it has shown that the more physiological 3D microenvironment probably induces specific metabolic pathways, related to cell differentiation and integrin-mediated cells' interaction with the substrate, instead of inducing a fast proliferation. It is in fact known that the lower number of cell doublings is associated with a progressive decrease in the osteogenic capacity of MSCs (Banfi et al, 2000 (48); Derubeis and Cancedda, 2004 (49); Sugiura et al, 2004 (50)).

After 2 weeks of subcutaneous implantation in rats, samples were harvested and histologically analyzed. No significant evidence of inflammatory response was detected for any scaffold for the entire period of observation (Fig. 9C), according to the histological assays. No foreign body reaction was observed; various types of cells, including fibroblasts, monocytes and lymphocytes, entered the scaffold and initiated the formation of new connective tissue (Fig. 9C).

Conclusion

A key current strategy in regenerative medicine is the critical study of natural tissues and biomimesis to inform the design of new composite materials able to emulate the structural and functional response of tissue.

In this study, a resorbable bilayered monolithic osteochondral graft purposely designed to prevent delamination of the 2 distinct layers (bone and cartilage) and, simultaneously, to provide the proper biochemical cues for efficient and selective generation of the 2 tissues was successfully realized. The highly porous scaffold prototype was obtained by freeze-drying a calcium cross-linked alginate-based hydrogel where HA was used as bioactive signal to induce osteogenic differentiation in the bony layer, and TGF-β1 to induce chondrogenesis in the cartilage layer containing alginate-sulfate as the growth factor binder.

The structural, chemical and biomechanical features of such a prototype were shown to offer a proper balance between the required mechanical properties and resorbability, while guaranteeing a microenvironment potentially permissive to in vivo cell-mediated matrix deposition.

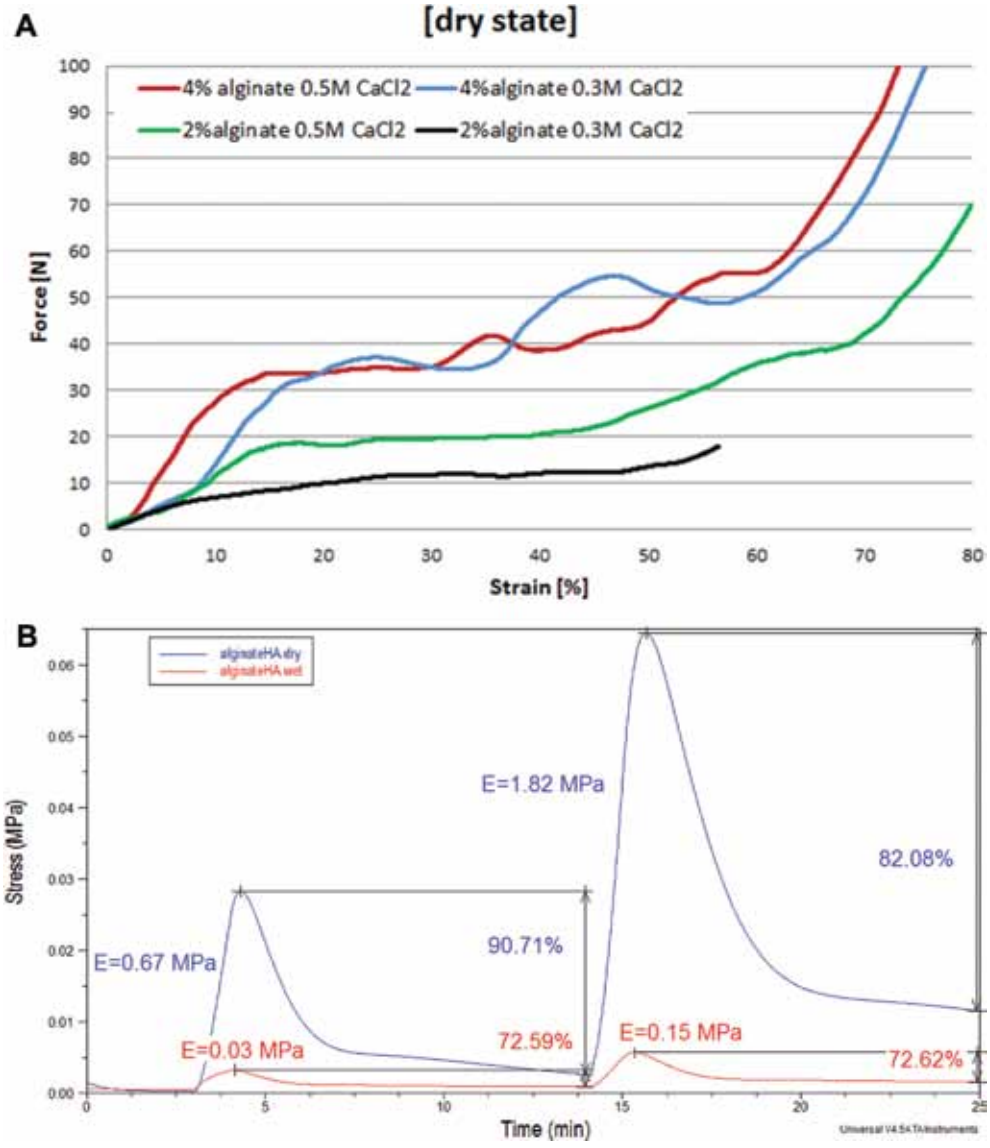

Fig. 8 - (**A**) Mechanical compression tests on the 4 typologies of freeze-dried scaffold; (**B**) stress relaxation tests on the dynamic mechanical analyzer (DMA) on the CaP scaffolds: the compressive modulus and the stress recovery ability per each sample are plotted on the graph.

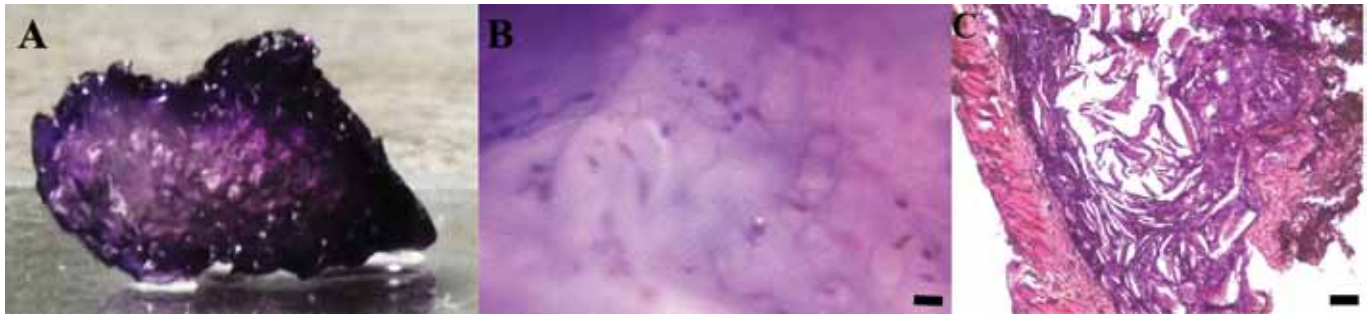

Fig. 9 - (**A, B**) Toluidine blue staining of the alginate scaffold seeded with mesenchymal stem cells (MSCs): (**A**) macro view of the spatial distribution of cells; (**B**) micro view of the cells spreading within the graft (scale bar 10 µm); (**C**) hematoxylin and eosin (H&E) staining after 2 weeks of subcutaneous implantation of the scaffolds in rat (scale bar 100 µm).

In vitro tests, carried out with MSCs, showed the absence of any cytotoxicity of the material, proving a good cell adhesion and cell–material interaction for up to 7 days, Moreover, in vivo experiments on rats led to no significant evidence of inflammatory phenomena provoked by the subcutaneously implanted scaffolds for the entire period of observation, thus

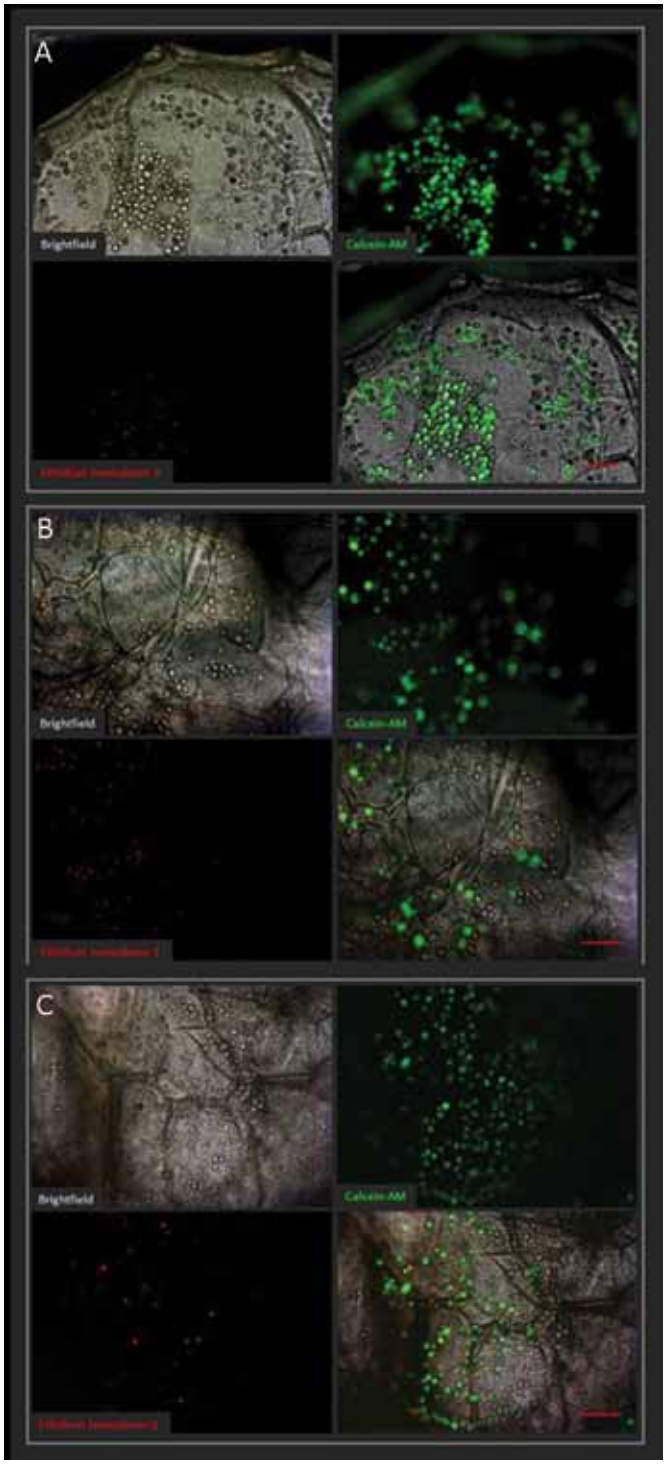

Fig. 10 - Viability tests (Live/Dead) for mesenchymal stem cells (MSCs) seeded on the alginate scaffold after 1 (**A**), 3 (**B**) and 7 days (**C**). The brightfield and the 2 different fluorescence channels (green and red) were merged to produce the composite final images; scale bar 100 μm.

confirming its suitability as an alternative scaffold for possible tissue regeneration applications.

The results achieved here demonstrated the efficacy of the presented approach to develop a highly porous bioactive osteochondral graft, which combines interesting functional properties and biomechanical performances, thus becoming a promising candidate for the treatment of articular joint defects. Future work could be addressed to the validation of the alginate-based scaffolds on prolonged periods of cell culture and in vivo implants in orthotopic model defects.

Acknowledgement

The authors wish to thank Zwick-Roell Italia for mechanical characterization, Dr. Ilaria Schizzi and Dr. Roberto Utzeri of CNR-ISMAC Genova for FTIR, TGA and SEM-EDX analysis, Dr. Matteo Lorenzoni for AFM maps, Project Interomics and PRIN (Prot. N. 2010L9SH3K 2013-2015) for financial support.

Disclosures

Financial support: Project Interomics and PRIN (Prot. N. 2010L9SH3K 2013-2015).
Conflict of interest: The authors declare that there are no conflicts of interest.

References

1. Bose S, Roy M, Bandyopadhyay A. Recent advances in bone tissue engineering scaffolds. Trends Biotechnol. 2012;30(10): 546-554.
2. Dankers PY, Harmsen MC, Brouwer LA, van Luyn MJ, Meijer EW. A modular and supramolecular approach to bioactive scaffolds for tissue engineering. Nat Mater. 2005;4(7):568-574.
3. Lenza RF, Vasconcelos WL, Jones JR, Hench LL. Surface-modified 3D scaffolds for tissue engineering. J Mater Sci Mater Med. 2002;13(9):837-842.
4. Jones JR, Ehrenfried LM, Hench LL. Optimising bioactive glass scaffolds for bone tissue engineering. Biomaterials. 2006;27(7):964-973.
5. Tampieri A, Sandri M, Landi E, et al. Design of graded biomimetic osteochondral composite scaffolds. Biomaterials. 2008;29(26):3539-3546.
6. Grayson WL, Chao PH, Marolt D, Kaplan DL, Vunjak-Novakovic G. Engineering custom-designed osteochondral tissue grafts. Trends Biotechnol. 2008;26(4):181-189.
7. Jiang J, Tang A, Ateshian GA, Guo XE, Hung CT, Lu HH. Bioactive stratified polymer ceramic-hydrogel scaffold for integrative osteochondral repair. Ann Biomed Eng. 2010;38(6): 2183-2196.
8. Lynn AK, Best SM, Cameron RE, et al. Design of a multiphase osteochondral scaffold: I. control of chemical composition. J Biomed Mater Res A. 2010;92(3):1057-1065.
9. Mano JF, Reis RL. Osteochondral defects: present situation and tissue engineering approaches. J Tissue Eng Regen Med. 2007;1(4):261-273.
10. Oliveira JM, Rodrigues MT, Silva SS, et al. Novel hydroxyapatite/chitosan bilayered scaffold for osteochondral tissue-engineering applications: scaffold design and its performance when seeded with goat bone marrow stromal cells. Biomaterials. 2006;27(36):6123-6137.
11. Hutmacher DW. Scaffolds in tissue engineering bone and cartilage. Biomaterials. 2000;21(24):2529-2543.
12. Rezwan K, Chen QZ, Blaker JJ, Boccaccini AR. Biodegradable and bioactive porous polymer/inorganic composite scaffolds for bone tissue engineering. Biomaterials. 2006;27(18): 3413-3431.

13. Wagoner Johnson AJ, Herschler BA. A review of the mechanical behavior of CaP and CaP/polymer composites for applications in bone replacement and repair. Acta Biomater. 2011;7(1): 16-30.
14. Altman GH, Diaz F, Jakuba C, et al. Silk-based biomaterials. Biomaterials. 2003;24(3):401-416.
15. Glowacki J, Mizuno S. Collagen scaffolds for tissue engineering. Biopolymers. 2008;89(5):338-344.
16. Liu X, Ma PX. Polymeric scaffolds for bone tissue engineering. Ann Biomed Eng. 2004;32(3):477-486.
17. Scaglione S, Lazzarini E, Ilengo C, Quarto R. A composite material model for improved bone formation. J Tissue Eng Regen Med. 2010;4(7):505-513.
18. Benya PD, Shaffer JD. Dedifferentiated chondrocytes reexpress the differentiated collagen phenotype when cultured in agarose gels. Cell. 1982;30(1):215-224.
19. Nicodemus GD, Bryant SJ. The role of hydrogel structure and dynamic loading on chondrocyte gene expression and matrix formation. J Biomech. 2008;41(7):1528-1536.
20. Chicatun F, Pedraza CE, Muja N, Ghezzi CE, McKee MD, Nazhat SN. Effect of chitosan incorporation and scaffold geometry on chondrocyte function in dense collagen type I hydrogels. Tissue Eng Part A. 2013;19(23-24):2553-2564.
21. Coates EE, Riggin CN, Fisher JP. Photocrosslinked alginate with hyaluronic acid hydrogels as vehicles for mesenchymal stem cell encapsulation and chondrogenesis. J Biomed Mater Res A. 2013;101(7):1962-1970.
22. Calvert P. Hydrogels for soft machines. Adv Mater. 2009;21(7): 743-756.
23. Giannoni P, Lazzarini E, Ceseracciu L, Barone AC, Quarto R, Scaglione S. Design and characterization of a tissue-engineered bilayer scaffold for osteochondral tissue repair. J Tissue Eng Regen Med. 2012;n/a.
24. Malafaya PB, Gomes ME, Salgado AJ, Reis RL. Polymer based scaffolds and carriers for bioactive agents from different natural origin materials. Adv Exp Med Biol. 2003;534: 201-233.
25. Oerther S, Payan E, Lapicque F, et al. Hyaluronate-alginate combination for the preparation of new biomaterials: investigation of the behaviour in aqueous solutions. Biochim Biophys Acta. 1999;1426(1):185-194.
26. Pawar SN, Edgar KJ. Alginate derivatization: a review of chemistry, properties and applications. Biomaterials. 2012;33(11): 3279-3305.
27. Draget KI, Smidsrød O, Skjåk-Bræk G. Alginates from Algae. Biopolymers Online. 2005: DOI: 10.1002/3527600035.bpol6008.
28. Häuselmann HJ, Masuda K, Hunziker EB, et al. Adult human chondrocytes cultured in alginate form a matrix similar to native human articular cartilage. Am J Physiol. 1996;271(3 Pt 1): C742-C752.
29. Gao J, Dennis JE, Solchaga LA, Awadallah AS, Goldberg VM, Caplan AI. Tissue-engineered fabrication of an osteochondral composite graft using rat bone marrow-derived mesenchymal stem cells. Tissue Eng. 2001;7(4):363-371.
30. Holland TA, Bodde EW, Baggett LS, Tabata Y, Mikos AG, Jansen JA. Osteochondral repair in the rabbit model utilizing bilayered, degradable oligo(poly(ethylene glycol) fumarate) hydrogel scaffolds. J Biomed Mater Res A. 2005;75(1): 156-167.
31. Kon E, Delcogliano M, Filardo G, et al. Orderly osteochondral regeneration in a sheep model using a novel nano-composite multilayered biomaterial. J Orthop Res. 2010;28(1):116-124.
32. Schaefer D, Martin I, Jundt G, et al. Tissue-engineered composites for the repair of large osteochondral defects. Arthritis Rheum. 2002;46(9):2524-2534.
33. Sherwood JK, Riley SL, Palazzolo R, et al. A three-dimensional osteochondral composite scaffold for articular cartilage repair. Biomaterials. 2002;23(24):4739-4751.
34. Goldring MB. Update on the biology of the chondrocyte and new approaches to treating cartilage diseases. Best Pract Res Clin Rheumatol. 2006;20(5):1003-1025.
35. Blom AB, van der Kraan PM, van den Berg WB. Cytokine targeting in osteoarthritis. Curr Drug Targets. 2007;8(2):283-292.
36. Yaeger PC, Masi TL, de Ortiz JL, Binette F, Tubo R, McPherson JM. Synergistic action of transforming growth factor-beta and insulin-like growth factor-I induces expression of type II collagen and aggrecan genes in adult human articular chondrocytes. Exp Cell Res. 1997;237(2):318-325.
37. Re'em T, Kaminer-Israeli Y, Ruvinov E, Cohen S. Chondrogenesis of hMSC in affinity-bound TGF-beta scaffolds. Biomaterials. 2011.
38. Sader JE, Chon JWM, Mulvaney P. Calibration of rectangular atomic force microscope cantilevers. Rev Sci Instrum. 1999; 70(10):3967-3969.
39. Mastrogiacomo M, Scaglione S, Martinetti R, et al. Role of scaffold internal structure on in vivo bone formation in macroporous calcium phosphate bioceramics. Biomaterials. 2006; 27(17):3230-3237.
40. Caykara T, Demirci S, Eroglu MS, Guven O. Poly(ethylene oxide) and its blends with sodium alginate. Polymer (Guildf). 2005;46(24):10750-10757.
41. Swamy TM, Ramaraj B, Siddaramaiah. Sodium alginate and poly(ethylene glycol) blends: thermal and morphological behaviors. J Macromol Sci Part A Pure Appl Chem. 2010;47(9):877-881.
42. Xiao CB, Lu YS, Liu HJ, Zhang LN. Preparation and physical properties of blend films from sodium alginate and polyacrylamide solutions. Journal of Macromolecular Science Pure and Applied Chemistry. 2000;37(12):1663-1675.
43. Pathak TS, Yun JH, Lee J, Paeng KJ. Effect of calcium ion (crosslinker) concentration on porosity, surface morphology and thermal behavior of calcium alginates prepared from algae (Undaria pinnatifida). Carbohydr Polym. 2010;81(3):633-639.
44. Freeman I, Kedem A, Cohen S. The effect of sulfation of alginate hydrogels on the specific binding and controlled release of heparin-binding proteins. Biomaterials. 2008;29(22): 3260-3268.
45. Sasisekharan R, Venkataraman G. Heparin and heparan sulfate: biosynthesis, structure and function. Curr Opin Chem Biol. 2000;4(6):626-631.
46. Ronghua H, Yumin D, Jianhong Y. Preparation and anticoagulant activity of carboxybutyrylated hydroxyethyl chitosan sulfates. Carbohydr Polym. 2003;51(4):431-438.
47. Chen A., Haddad D., Wang R. Analysis of chitosan-alginate bone scaffolds. Rutgers University, New Jersey Governor's School of Engineering & Technology, 1-8.
48. Banfi A, Muraglia A, Dozin B. Mastrogiacomo M, Cancedda R. Quarto B. Proliferation kinetics and differentiation potential of ex vivo expanded human bone marrow stromal cells: Implications for their use in cell therapy. Experimental Hematology 28. (2000);707-715.
49. Derubeis AR, Cancedda R. Bone marrow stromal cells (BMSCs) in bone engineering: limitations and recent advances. Ann Biomed Eng. 2004;32(1):160-5.
50. Sugiura F, Kitoh H, Ishiguro N. Osteogenic potential of rat mesenchymal stem cells after several passages. Biochem Biophys Res Commun. 2004;316(1):233-239.